Heliyon 10 (2024) e38892

Contents lists available at ScienceDirect

Heliyon

journal homepage: www.cell.com/heliyon

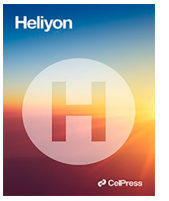

Research article

Mesoporous activated carbon derived from Chinese herbal medicine residues for hemoperfusion removal of uremia toxins from progressive chronic kidney diseases patients

Chengyu Yang [a,1], Lipeng Diao [c,1], Zhuo Song [a], Chen Guan [a], Lingyu Xu [a], Quandong Bu [a], Wei Jiang [a], Huiqing Yu [b,2], Daohao Li [c,*,2], Yan Xu [a,2]

[a] Department of Nephrology, The Affiliated Hospital of Qingdao University, Qingdao, 266003, PR China
[b] School of Basic Medicine, Qingdao University, Qingdao, 266071, PR China
[c] State Key Laboratory of Bio-fibers and Eco-textiles, College of Materials Science and Engineering, Qingdao University, Qingdao, 266071, PR China

ARTICLE INFO

Keywords:
Hemoperfusion
Activated carbon
Chinese herbal medicine residues
Uremia toxins

ABSTRACT

Hemoperfusion is one of the most important therapies for progressive chronic kidney disease (CKD) and is effective at removing toxins from the blood. Increasing the efficiency of adsorbents applied in hemoperfusion is crucial. In the present study, shell of areca nut, one of the most common waste Chinese herb medicine residue with a porous structure was carbonized and activated at different temperatures to obtain two kinds of porous materials. The biocompatibility of the as-prepared porous materials was estimated via a hemolytic test, and the removal efficiency of the materials toward toxins was tested via an adsorption experiment in solution and blood samples from CKD patients, simulated hemoperfusion and in vivo hemoperfusion. After 4 h of adsorption, free and protein-bound toxins in solution were efficiently removed by the prepared porous materials, and the removal efficiency was better than that of commonly used hemoperfutor adsorbents. Most of the tested toxins can be removed from CKD blood samples and simulated hemoperfusion samples. Blood uremic toxins from CKD mice were also efficiently and safely removed after in vivo hemoperfusion using the as-prepared adsorbent. This work highlights promising adsorbents for hemoperfusion that could increase the therapeutic efficacy in patients with progressive CKD.

1. Introduction

Kidney replacement therapy (KRT), the main treatment approach for kidney failure, saves millions of lives. In 2010, approximately 2.6 million patients received KRT worldwide; however, the number of patients who needed KRT was as high as 9.6 million [1], indicating that millions of people died because of the lack of opportunities to receive KRT [2]. Unfortunately, the number of patients who cannot receive prompt KRT will continue to increase and may reach as high as 9.4 million by 2030. Hemoperfusion is an important kind of KRT that is effective at removing serum creatinine (Scr) and mesomolecular and macromolecular toxins [3]. During

* Corresponding author.
E-mail addresses: yuhuiqing@qdu.edu.cn (H. Yu), lidaohao@qdu.edu.cn (D. Li), xuyan@qdu.edu.cn (Y. Xu).
[1] C. Yang and L. Diao contribute equally to this work.
[2] Huiqing Yu, Daohao Li and Yan Xu contribute equally to this work.

https://doi.org/10.1016/j.heliyon.2024.e38892
Received 13 January 2024; Received in revised form 3 September 2024; Accepted 1 October 2024
Available online 2 October 2024

hemoperfusion, toxins such as Scr, interleukin-6 (IL-6) and parathyroid hormone (PTH) from the blood are eliminated by the adsorbents in the container [4]; thus, the performance and hemocompatibility of the adsorbents determine the curative efficiency of hemoperfusion [5,6]. To allow more patients to receive hemoperfusion, the efficiency of hemoperfusion must be increased, especially by improving the materials applied in hemoperfusion.

Since the first hemoperfusion model was described in 1964, different kinds of nanomaterials have been used as adsorbents for hemoperfusion. Activated carbon has become a universal adsorbent with a long history of application [7]; nonetheless, traditional activated carbon (TAC) displays indiscriminate adsorption ability, and its nanopores are too small to efficiently remove protein-bound toxins [8,9]. Although other adsorbents, such as some zeolites and some other polymers, have ideal affinities for specific targeted toxins, the capacities of these adsorbents are not as high as expected; moreover, unlike activated carbons, polymer-based adsorbents cannot be activated, which limits their inner pore accessibility and results in limitations of their functional surface area [10,11]. To improve the adsorption efficiency, activated carbons synthesized from different raw materials, such as activated carbons made from waste cigarettes, plant seeds and sawdust, have been employed as toxin adsorbents. These activated carbons are carbonized from natural raw materials, ensuring good biocompatibility [12–14]. In addition, recycling these raw materials can solve waste management problems. Chinese herbal medicine residues (CHMRs) are new kinds of raw materials. In China, approximately 70 million tons of waste CHMRs are generated each year, which leads to environmental problems. To solve environmental problems, CHMRs have been used as raw materials for sewage treatment, compost and renewable energy [15]. The thermochemical conversion of CHMRs can generate biochars, which are advanced materials with high removal efficiency and adsorption capacity [16]. Unlike other natural raw materials of activated carbons, after decocting, drug molecules separated from traditional Chinese medicinal materials and poses are already formed before carbonization. These characteristics make CHMRs ideal raw materials for synthesizing activated carbons for use in hemoperfusion. Because of the wide range of available raw materials, the cost of synthesizing activated carbons from CHMRs is very low, and hemoperfusion using adsorbents derived from CHMRs causes no additional burden on CKD patients [17].

The shell of the areca nut is a widely used traditional Chinese medicine that is multifibrous and is an ideal raw material for synthesizing activated carbons with a high specific surface area. In this study, the shell of areca nut plants was used as a raw material. By carbonizing and activating shell of areca nut, we synthesized different kinds of nanomaterials that were porous and possessed large surface areas (3077.96 m^2/g and 2667.36 m^2/g). We first confirmed the biocompatibility of the as-prepared biochar materials. After 4 h of adsorption, most of the different toxin simulators including phenol red (PR), vitamin B12 (VB_{12}) and protein-bound PR (p-PR) in solution were removed. Then, these biochar materials were added to the blood samples of progressive CKD patients, and Scr, PTH and IL-6 were efficiently removed by the as-prepared adsorbents. Furthermore, these porous materials were packed into a simulated hemoditoxifier, and IL-6 and Scr were efficiently removed via simulated hemoperfusion or hemoperfusion in vivo. Our work verified that the as-prepared porous biochar materials are valuable adsorbents for hemoperfusion.

2. Materials and methods

2.1. Synthesis of activated carbons using shell of areca nut

First, the biomass raw material was ground, and the powder was sieved. Then, the powder was heated to 400 °C or 700 °C at a heating rate of 1 °C/min and kept at 400 °C or 700 °C for 1 h. The carbonized powder was mixed with KOH powder at a ratio of 1:4. Afterward, the mixed powder was heated to 800 °C at a heating rate of 5 °C/min and kept at 800 °C for 0.5 h. After cooling to room temperature, the obtained powder was soaked in 3 mol/L hydrochloric acid solution for 12 h. Two kinds of powders were obtained after washing and drying and were labeled 400/800 and 700/800.

2.2. Characterization

XRD was conducted using a SmartLab-SE X-ray diffractometer at 40 kV and 40 mA equipped with Cu Kα radiation. Morphological and structural investigations were conducted by means of scanning electron microscopy (SEM, TESCAN MIRA LMS) at 3 kV and transmission electron microscopy (TEM, FEI Talos F200x G2) at 200 kV. A Thermo Scientific K-Alpha electron spectrometer was used for X-ray photoelectron spectroscopy (XPS) with Al Ka radiation (hv = 1486.6 eV). Raman spectra were obtained using a LabRAM HR evolution instrument with a 514 nm excitation wavelength. Surface functional groups were determined by Fourier transform infrared (FTIR) spectroscopy using a Nicolet iS20 spectrometer. The porosity of the prepared materials was determined via physical adsorption of N_2 at 77 K via an ASAP2460 automatic specific surface area analyzer, and the specific surface area of the samples was determined via the BET method.

2.3. Hemolysis evaluation

Red blood cells (RBCs) were collected from a healthy volunteer in the laboratory by centrifuging the blood at 3000 rpm for 10 min and removing the supernatant. The collected RBCs were then washed three times and diluted to 2 % in phosphate-buffered saline (PBS). The prepared materials at different concentrations were added to the RBC suspension and incubated at 37 °C for 30 min. RBC samples diluted with PBS were used as a negative control (NC), while those diluted with distilled water were used as a positive control (PC). After incubation, the RBC samples were obtained by centrifugation at 1000 rpm for 10 min. The absorbance of the obtained samples at 541 nm was measured. The hemolysis ratio (%) of the as-prepared materials was calculated by the following equation:

Hemolysis ratio (%) = $[(A_n\text{-}A_{NC})/(A_{PC}\text{-}A_{NC})] \times 100$ %, where A is the absorbance at 541 nm of the tested sample (A_n), the negative

control (A_{NC}) or the positive control (A_{NC}).

2.4. Removal efficiency of PR and VB_{12} in PBS

To evaluate the adsorption kinetics of PR and VB_{12}, solution samples of PR or VB_{12} with initial concentrations of 30 mg/L and 200 mg/L, respectively, were prepared by dissolving PR or VB_{12} powder in PBS. The as-prepared materials were subsequently added to the PR or VB_{12} solution samples. The suspended samples were shaken at 175 rpm at 37 °C. The supernatants of the samples were collected, and the PR supernatants were mixed with 1 M NaOH at a ratio of 1:1. The absorbency at 560 nm or 360 nm was measured at different time points using an ultraviolet spectrophotometer (Thermo Fisher Scientific) to determine the residual concentration of PR or VB_{12}. The removal efficiency of the as-prepared materials for PR and VB_{12} was calculated by the following equation:

$$\text{removal efficiency}\ (100\%) = [(C_0\text{-}C_n) / C_0] \times 100\%$$

where C_0 is the initial concentration of the tested samples and C_n is the residual concentration at different time points.

2.5. Removal efficiency toward protein-bound PR

To explore the removal efficiency of protein-bound PR, a solution containing 40 mg/ml bovine serum albumin (BSA) and 30 mg/L PR was prepared. The prepared materials at a certain dose were added to the mixed solution. After shaking at 37 °C and 175 rpm, 150 μL of each supernatant was collected at different time points. Then, 450 μL of acetone was added to these samples, and the samples were fully mixed for 30 s. Finally, the supernatants without BSA were collected after centrifugation at 3000 rpm for 15 min. To determine the residual concentration of PR, the PR supernatants were mixed with 1 M NaOH at a ratio of 1:1, and the absorbance at 560 nm was measured. The removal efficiency toward PR was calculated as described above.

2.6. Adsorption of uremic toxins in the blood of CKD patients

Three stage 5 CKD patients were selected as volunteers to donate blood samples to test the efficiency of uremic toxin removal by the

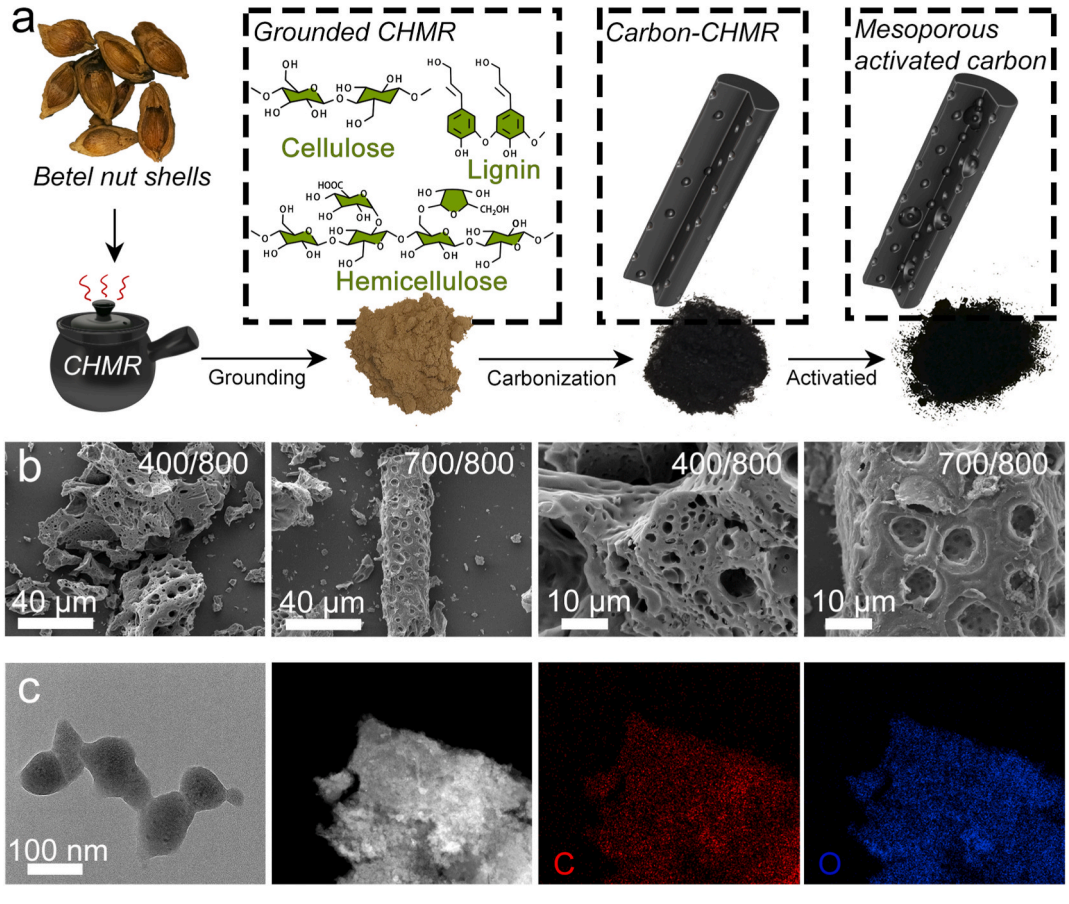

Fig. 1. Synthetic process (a), SEM image (b), TEM image and EDS map (c) of the as-prepared materials. The experiments were repeated three times.

as-prepared materials. The patients were fully informed that the study complied with Chinese ethical regulations and was approved by the Ethics Committee of the Affiliated Hospital of Qingdao University. Blood samples were collected as described above and diluted 10 times. Then, the as-prepared materials were added to those samples and shaken at 175 rpm at 37 °C for different durations. Then, the samples were centrifuged at 3000 rpm for 15 min to obtain the final samples. These samples were loaded into a Cobas Electrochemiluminescence Automatic Immunoanalyzer e411 or HITACHI Automatic Analyzer 7600, and the concentrations of parathyroid hormone (PTH), interleukin 6 (IL-6) and Scr were detected using electrochemiluminescence or a chemiluminescence immunoassay assay with Automatic Analyzer 7600 Scr exclusive reagent or texting kits (Roche 11972103122 and 05109442190).

2.7. *In vivo hemoperfusion*

CKD models of male SD rats (6–8 weeks) were established by 5/6 nephrectomy according to a previously described method [18]. All the animal studies were approved by the Ethics Committee of Qingdao University (202208SD33202306045). To narcotize the SD rats with CKD, 3.5 % chloral hydrate at 1 mL/100 g body weight was injected into the rats. After skin preparation, the abdominal aorta and postcava were dissected, and intravenous indwelling catheters were placed into the aortaventralis. Intravenous indwelling catheters were connected to tubing that was previously filled with 0.1 % sodium heparin-physiological saline solution. A total of 700/800 was loaded in a cartridge connected to the rat. A micro pump was used to drive blood flow. Before hemoperfusion, a 2.5 mg/100 g body weight heparin sodium solution was injected into the blood circulation. Then, hemoperfusion started with a 12 ml/min flow rate at pH 7.8 and a temperature of 36–37 °C. Blood and different organ samples were collected after hemoperfusion. Toxin concentrations were tested via an ELISA kit (Abcam, ab234570), and tissue injury levels were evaluated via hematoxylin-eosin (HE) staining.

2.8. *Statistical analysis*

Data from experiments were analyzed by a *t*-test for comparisons between two groups or by ANOVA for comparisons among multiple groups. Origin (OriginLab Inc.) was used to perform all statistical calculations ($p < 0.05$ was considered statistically significant) and create the histograms and line charts. The value shown in figures is an average value ± standard deviation.

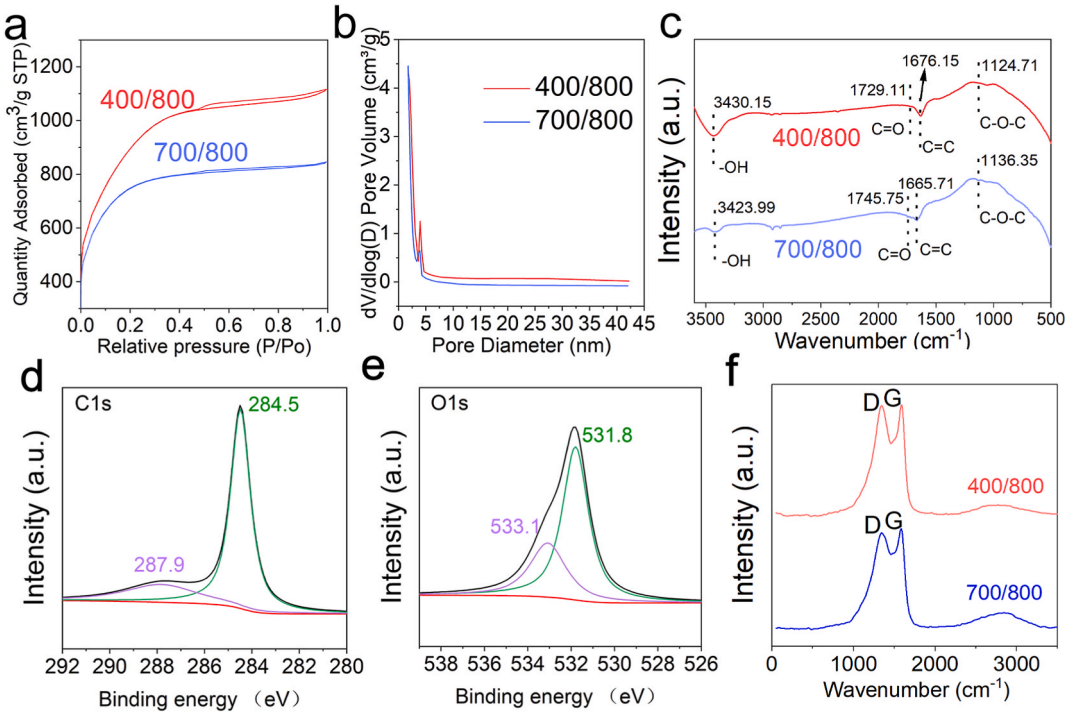

Fig. 2. Pore structure and pore size distribution (a, b), FTIR spectrum (c), Raman pattern (d), XPS pattern (e, f) and XRD patterns (g, h) of the as-prepared materials. The experiments were repeated three times.

3. Results

3.1. Characterization

Mesoporous activated carbons were successfully synthesized from the shell of areca nuts (Fig. 1a). After carbonization and activation, the biocompatibility of raw powder was improved (Fig. S1). Hemoditoxifier allergy is one of the leading causes of heart arrest in hemodialysis patients [19]. Thus, such a synthetic process ensures the safety of hemoperfusion. The morphology of the as-prepared materials was determined by SEM and TEM. As shown in Fig. 1b and c, both 400/800 and 700/800 had smooth surfaces and porous structures. Energy dispersive X-ray spectroscopy (EDS) maps showed the uniform distribution of C and O in the as-prepared materials. Fig. 2a and b illustrates the pore structure and pore size distribution of 400/800 and 700/800. Both the as-prepared samples showed type IV isotherms, indicating that these biomass materials possessed mesoporous structures. In addition, the pore volume peaks of 400/800 and 700/800 were approximately 3∼4 nm, and 400/800 exhibited a larger pore volume than 700/800, as determined via BET analysis. These results indicated a predominance of mesopore structures of 400/800 and 700/800, and the pore size was larger than that of TAC (less than 2 nm). Dozens of studies have shown that pore size is crucial for toxin removal efficiency, especially for removing medium and macromolecular toxins. In addition, the BET surface areas of 400/800 and 700/800 are 3077.96 m^2/g and 2667.36 m^2/g, respectively, both of which are larger than those of TAC and some modern activated carbons. The mesoporous structure and large surface area of 400/800 and 700/800 ensured the removal efficiency of larger-volume uremia toxins, such as IL-6, PTH and protein-bound toxins. The IR spectra of the as-prepared materials are shown in Fig. 2c. The absorption peaks at 3441.15 cm^{-1} and 3492.75 cm^{-1} were clearly observed in the IR spectra of 400/800 and 700/800, respectively, and these peaks were attributed to the stretching vibrations of –OH, which indicated the presence of alcoholic or phenolic hydroxyl groups. The 1676.15 cm^{-1} peak in the 400/800 spectrum and the 1656.14 cm^{-1} peak in the 700/800 spectrum corresponded to C=C, the 1799.11 cm^{-1} peak in the 400/800 spectrum and the 1747.21 cm^{-1} peak in the 700/800 spectrum corresponded to C=O, and the 1188.64 cm^{-1} peak in the 400/800 and the 1178.85 cm^{-1} peak in the 700/800 spectra were attributed to the stretching vibration of C-O-C [20]. The Raman spectra of the prepared activated carbons are shown in Fig. 2d. Peaks corresponding to the D and G bands were detected, and the I_D/I_G ratio of 400/800 was approximately 0.99, which was higher than that of 700/800 (0.96). These results indicated that 400/800 had more structural defects. Fig. 2e and f shows the XPS survey spectrum of 700/800. The C1s spectrum was deconvoluted into two peaks at 284.5 eV and 287.9 eV, corresponding to C=C and C-OH/C-O, respectively, while the O1s spectrum exhibited two major peaks at 531.8 eV and 533.1 eV, which were attributed to C=O and –OH, respectively [21]. The crystal structure and phase composition of the 400/800 and 700/800 samples were determined by X-ray diffraction (XRD), and the results are displayed in Fig. 2g and h. The XRD pattern presented diffraction peaks at approximately 27° and 44° for 400/800 and at 26° and 45° for 700/800, which were attributed to the (002) and (100) planes of the carbon materials, respectively. There were many defects on the carbon wall after the activation process, as determined from the TEM and BET results. In this case, the XRD diffraction peaks of 400/800 and 700/800 were relatively weak, and these weak XRD peaks of the as-prepared materials indicated that 400/800 and 700/800 had porous structures and high surface areas, consistent with previous results.

3.2. Hemolysis evaluation

Good hemocompatibility is one of the critical requirements for blood contact materials. Therefore, the hemolysis rates of the as-prepared materials were evaluated before the materials were used in blood, and the results are shown in Fig. 3a and b. Both 400/800 and 700/800 exhibited suitable HRs (no more than 5 %) at concentrations ≤1.5 mg/ml, and 400/800 induced less hemolysis than 700/800 at 1.5 mg/ml. Thus, 400/800 and 700/800 (concentration ≤1.5 mg/ml) were regarded as potential adsorbents for the removal of uremic toxins.

3.3. Removal efficiency of VB_{12}, PR and p-PR in solution

VB_{12} is a representative of middle molecular toxins and VB_{12} concentration is a commonly used adsorption indicator [22]. To evaluate their adsorption efficiency, 400/800 and 700/800 were added to a VB_{12} solution. After 0.5 h, approximately 28 % of the VB_{12}

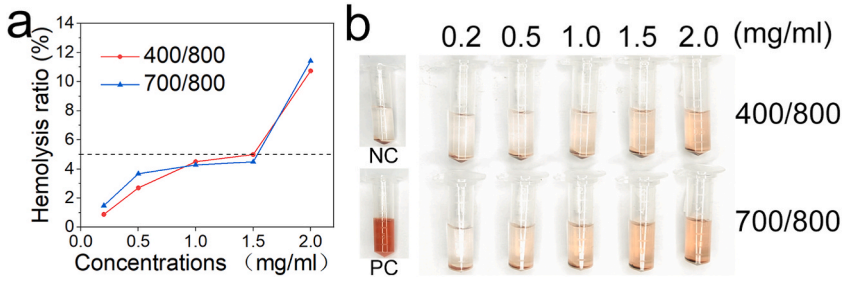

Fig. 3. Hemolysis evaluation. (a) Hemolysis ratios of as-prepared materials. The experiments were repeated three times. (b) Pictures of hemolysis evaluation.

was removed by 400/800, while approximately 40 % of the VB_{12} was removed by 700/800. The removal efficiency toward VB_{12} of both materials continually increased for 4 h, and 700/800 displayed a higher removal efficiency than 400/800 at all tested time points. The maximal removal efficiency of 400/800 was 81 %, while that of 700/800 was 82 %, and the absorption efficiency of both materials peaked at 4 h (Fig. 4a and b). The high VB_{12} removal efficiency indicated that both 400/800 and 700/800 are ideal adsorbents for middle-molecule toxins.

PR is a small-molecule toxin mimic, and its removal efficiency is considered an important factor in the evaluation of hemoperfusion adsorbents, especially in modeling the effect of protein binding on solute clearance [23,24]. In this study, the removal efficiency of the as-prepared materials for PR was tested. As shown in Fig. 4c andd, 400/800 removed approximately 76 % of the PR, while 700/800 removed approximately 77 % of the PR in only 0.5 h. The PR removal efficiency increased continually and peaked at 3 h. The maximum PR removal efficiencies of 400/800 and 700/800 were 78.2 % and 78.7 %, respectively. The removal rate of PR by the as-prepared materials was better than that of TAC at all time points except 2 h (Fig. 4c). The PR removal efficiency of HA230 (a commonly used adsorption resin) was also evaluated, as shown in Fig. 5a. After 4 h of adsorption, only approximately 12 % of the PR was removed by 1.5 mg/ml HA230, indicating that the as-prepared materials were more efficient than HA230 toward PR at the same concentration, which confirmed that the as-prepared materials can increase the adsorption efficiency toward small molecule toxins.

Protein-bound toxins are among the major macromolecular toxins that play important roles in pathophysiologic processes in CKD, and the accumulation of these solutes can aggravate complications. However, conventional hemodialysis results in a low reduction in protein-bound toxins, and hemoperfusion is a crucial way to remove protein-bound toxins [25]. To evaluate the protein-bound toxin removal efficiency of the as-prepared materials, PR was added to BSA, and 400/800 and 700/800 were added to p-PR. After 0.5 h, approximately 42 % of the p-PR was removed by 700/800, while approximately 35.4 % was removed by 400/800. However, these two materials displayed similar p-PR removal efficiencies at 1 h (approximately 54 %), and 400/800 removed more p-PR than 700/800 at 2 h, 3 h and 4 h. Such removal efficiency variance was attributed to the different pore sizes of the as-prepared materials. The removal efficiency of p-PR was lower than that of PR at all time points. These results indicated that this type of toxin is difficult to remove when bound to protein; however, the removal efficiency towards protein-bound toxins of the as-prepared materials is significantly increased compared with TAC (Fig. 4e and f). The maximal p-PR removal efficiencies of 400/800 and 700/800 were 65 % and 63 %, respectively,

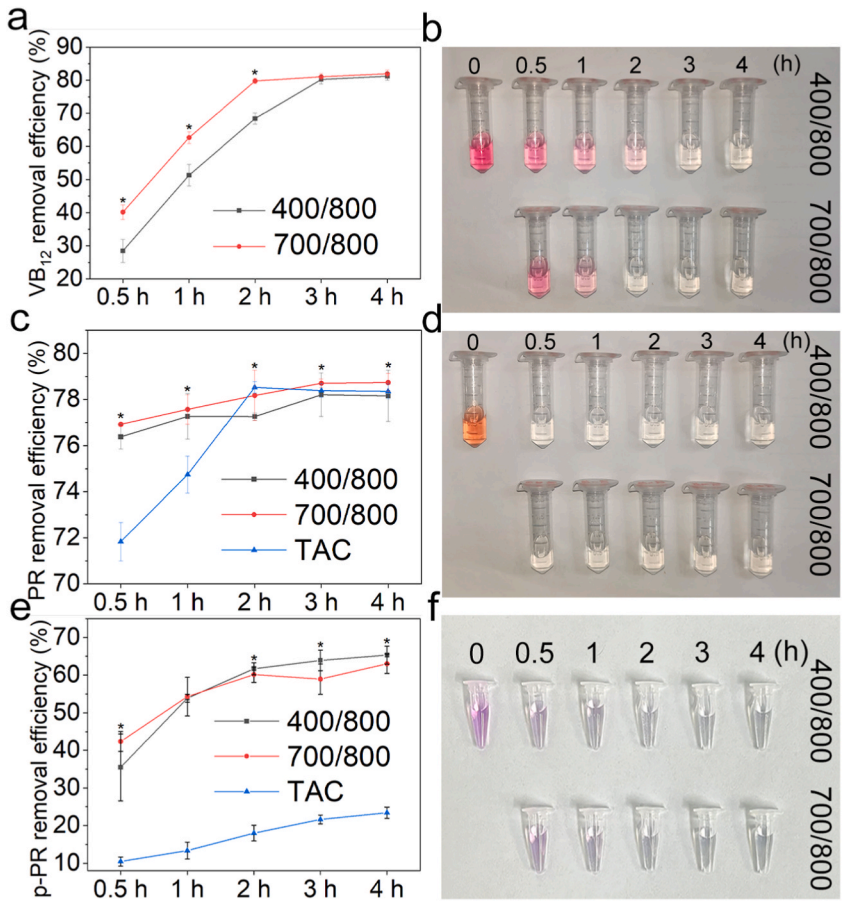

Fig. 4. Removal efficiency toward VB_{12} (a, b), PR (c, d) and p-PR (e, f). The experiments were repeated three times, *p < 0.05 compared with another group of as prepared material.

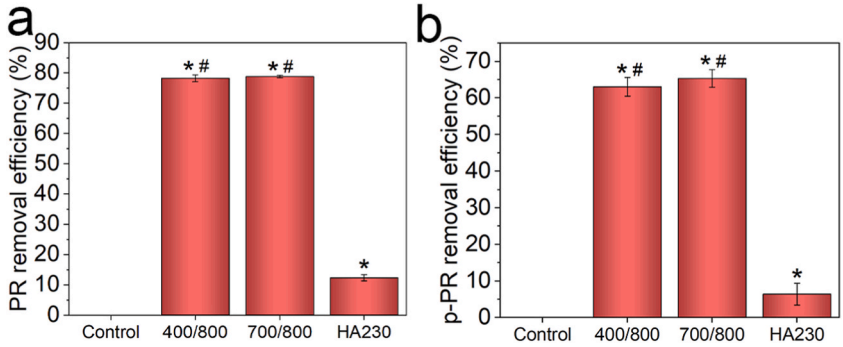

Fig. 5. PR (a) and p-PR (b) removal efficiencies of as-prepared materials and HA230. The experiments were repeated three times, *p < 0.05 compared with control group. #p < 0.05 compared with HA230 group.

both of which are higher than that of H103 according to a previous study (9). Furthermore, the p-PR removal efficiency of HA230 was also tested. As shown in Fig. 5b, the p-PR removal efficiency of the as-prepared materials was greater than that of HA230 at 1.5 mg/ml. The above results indicated that the as-prepared activated carbons maintained a similar adsorption efficiency for small-molecule toxins as TAC but displayed a higher removal efficiency for protein-bound toxins than TAC. These advantages of 400/800 and 700/800 were attributed to their larger pore sizes than TAC and larger surface areas than commonly used resins. In addition, the as-prepared activated carbons can also remove free PR molecules from albumin, resulting in more PR molecules being released from the PR-protein complexes; this mechanism can also improve the clearance efficiency of p-PR [26].

3.4. Removal efficiency of PTH, IL-6 and Scr in blood samples of CKD patients

Calcium-phosphorus homeostasis failure is one of the most serious complications in CKD patients and may result in hypocalcemia and hyperphosphatemia and ultimately increase PTH release via the calcium-sensing receptor on parathyroid cells. A high level of PTH in the human body increases the risk of bone disorders and angiogenesis [27]. PTH is one of the most common mesomolecular toxins in the blood of hemodialysis patients, and the PTH removal efficiency of the as-prepared materials was tested in blood samples from three CKD patients. As shown in Fig. 6a, both 400/800 and 700/800 absorbed most of the PTH in blood samples of CKD patients at 1 h, and the PTH levels continued to decrease during the continuous test. 700/800 displayed a faster adsorption rate than 400/800, as it removed approximately 63 % of the PTH in 1 h, while 400/800 removed only approximately 58 % at the same time point. However, 400/800 removed as much as 67 % of the PTH, and 700/800 removed no more than 65 % of the PTH at 3 h, indicating that 400/800

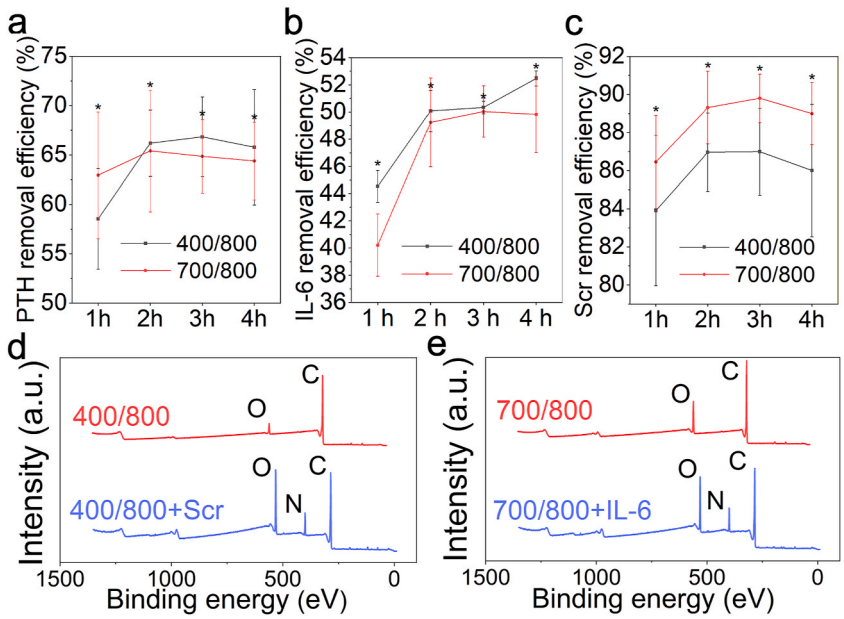

Fig. 6. Removal efficiency of PTH (a), IL-6 (b) and Scr (c) in CKD patients and XPS patterns of fresh and used as-prepared materials (d, e). The experiments were repeated three times, *p < 0.05 compared with another group of as prepared material.

had a greater adsorption capacity than 700/800 for mesomolecular toxins. In addition, 1.5 mg/ml of both 400/800 and 700/800 was more efficient at removing PTH than was HA-130 (a frequently used resin in hemoperfusion), according to a previous study [28]. IL-6 is another common mesomolecular toxin in the blood of CKD patients who may lead to a series of inflammatory reactions and ultimately aggravated kidney injury. Moreover, IL-6 is also a crucial cytokine for cardiovascular events in patients with CKD [29]. Adsorption of IL-6 by hemoperfusion has been the focus of dozens of studies, as uncontrolled release of IL-6 is associated with high mortality in many kidney diseases. Owing to its large size, IL-6 is difficult to remove via dialytic techniques. Legacy microporous sorbents have shown some effectiveness in the extraction of IL-6; however, their efficiency is poorer than that of mesoporous sorbents [30]. The removal efficiency of IL-6 was tested in the present study. As shown in Fig. 6b, approximately 44 % and 41 % of the IL-6 was removed by 400/800 and 700/800, respectively, in 1 h. The IL-6 removal efficiency of 400/800 continually increased over 4 h. Furthermore, 400/800 removed as much as 52 % of the IL-6 in 4 h, while 700/800 absorbed up to 50 % of the IL-6 in 3 h. These results confirmed the high adsorption efficiency of the as-prepared materials toward mesomolecular toxins. After absorption, the N peak was detected by XPS, but this peak was not detected in the fresh 700/800 sample. These XPS results confirmed that IL-6 was adsorbed by the as-prepared active carbons (Fig. 6d). Furthermore, 400/800 and 700/800 removed approximately 84 % and 86 %, respectively, of the total soluble protein (Scr) in 1 h, and the Scr removal efficiency of both materials continued to increase over time and reached 87 % and 90 %, respectively, at 3 h (Fig. 6c). The XPS patterns also confirmed that Scr was absorbed by the as-prepared active carbons (Fig. 6e). According to our results, 400/800 was more efficient at removing mesomolecular toxins from CKD blood samples, while 700/800 displayed high adsorption efficiency toward small-molecule toxins, consistent with the BET results and toxin removal efficiency in solution.

3.5. Removal efficiency of PR and IL-6 via simulated hemoperfusion

The above results indicated the potential of activated carbons synthesized from shell of areca nut as promising nanomaterials for toxin adsorption in static liquids. However, hemoperfusion is a dynamic process. To evaluate the dynamic toxin removal efficiency of the as-prepared materials, 700/800, which displayed the highest adsorption capacity, was loaded in a single-use filter unit and connected via a hemoperfusion pathway. A peristaltic pump was used to launch simulated hemoperfusion, and the removal efficiency was determined in a single liquid cycle. As shown in Fig. 7a–d, after hemoperfusion, as much as 95 % of the PR was efficiently removed by 700/800 according to the absorbance at 560 nm, while the filter without the as-prepared materials removed only approximately 5 % of the PR. This result confirmed the adsorption capacity of 700/800 toward toxins in flowing liquid. Furthermore, such hemoperfusion using 700/800 also removed approximately 45 % of the IL-6 in a single liquid cycle (Fig. 7e). These results confirmed the high uremic toxin removal efficiency of 700/800 and provided the basis for in vivo hemoperfusion.

3.6. Hemoperfusion in vivo

The above results confirmed the advantages of the as-prepared materials in simulated hemoperfusion, and the toxin removal efficiency of the as-prepared materials was subsequently evaluated in vivo. A chronic renal failure animal model was successfully established according to the Scr level. The hemoperfusion unit was connected to CKD rats (Fig. 8a and b). After modeling, the Scr level of the tested rats was upregulated compared to that of the control rats, while after 15 min of hemoperfusion, the Scr level was significantly decreased (Fig. 8c). Organs such as the liver, heart, spleen and lung with abundant blood flow are vulnerable to KRT. After hemoperfusion, the rats were sacrificed, and organ samples were collected. As shown in Fig. 8d and e, after hemoperfusion, no tissue injury was detected in the heart, liver, spleen or lung samples. These results indicated that 700/800 is an ideal material for hemoperfusion.

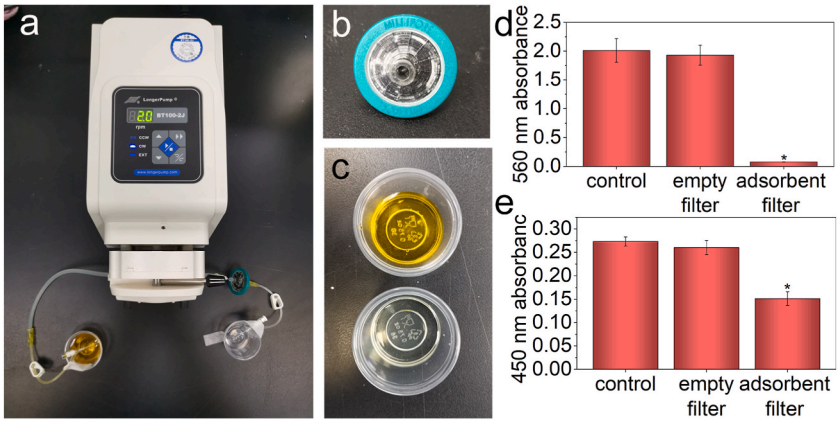

Fig. 7. Simulated hemoperfusion unit (a, b) and removal efficiency toward PR (c, d) and IL-6 (e) via simulated hemoperfusion. The experiments were repeated three times, *p < 0.05 compared with empty filter group.

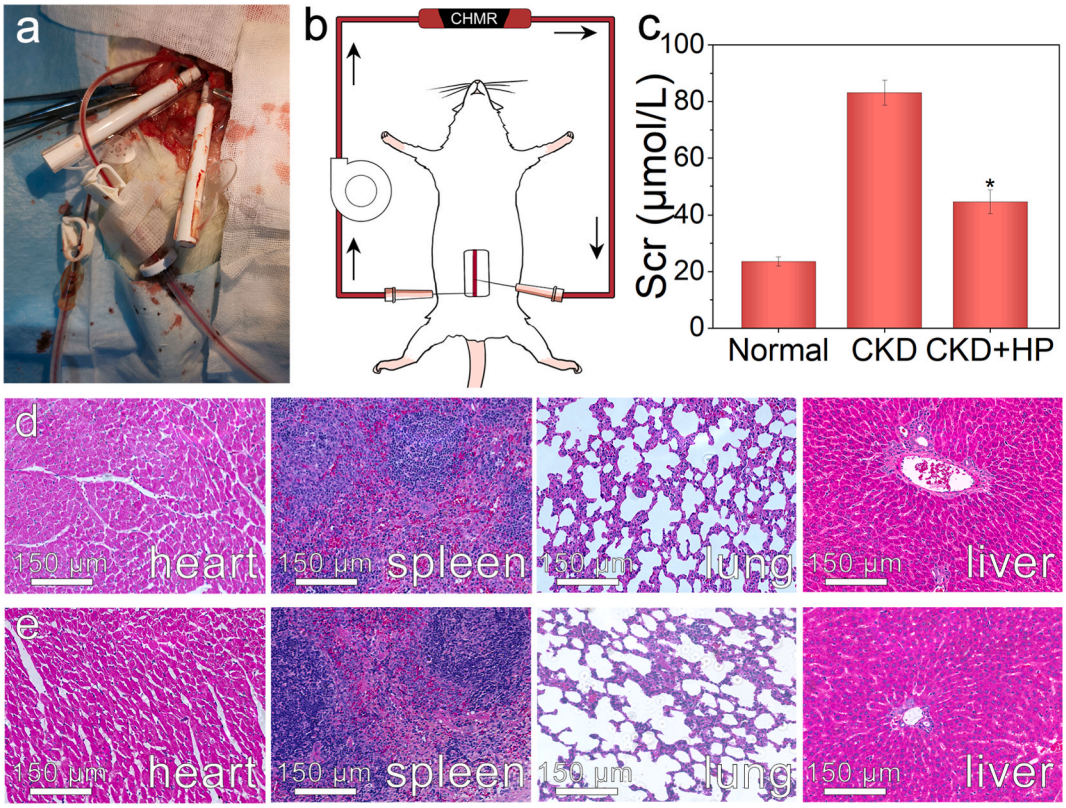

Fig. 8. Unit (a), schematic diagram (b) of in vivo hemoperfusion and Scr levels (c) and HE staining patterns (d, e) of CKD rats before and after in vivo hemoperfusion. The experiments were repeated three times, *p < 0.05 compared with CKD group.

4. Discussion

Hemoperfusion is a therapeutic method to absorb toxins in blood purification and adsorbents determine the efficacy of hemoperfusion. Activated carbon is a common adsorbent for hemoperfusion with long history of application. In order to improve the toxin removal efficiency of hemoperfusion, two new kinds of activated carbon were synthesized from betel nut shells. Compared with some other activated carbons, the synthesis method of as-prepared materials is more simplified [31]. After carbonization and activation, the hemolysis ratio of as-prepared materials is significant decline compared with raw powder. This maybe because some of toxic molecule are removed during high temperature process [32,33]. Pore size and surface area of activated carbons are key factors in toxins adsorption [22], in present study, as-prepared materials has lager pore size and surface area than TAC and some other activated carbons according to BET test which guaranteed their better adsorb ability towards toxins [22]. The toxin removal efficiency was firstly tested in solution. PR, VB_{12} and p-PR are commonly used small molecular, middle molecular and macromolecular toxin mimic and both of as-prepared materials can effectively remove those toxin mimics in solution which indicated good ability of 400/800 and 700/800 in removing toxins of different sizes. Besides, the removal efficiency of as-prepared activated carbons towards PR and p-PR is better than HA230, a commonly used resin in hemoperfusion. Due to poor renal function and different pathogenesis of CKD patients, the levels of proinflammatory factors, cytokines and metabolites in the blood of CKD patients are elevated and cannot be effectively eliminated [34,35]. IL-6, PTH, Scr and β2-microglobulin are typical uremia toxins that many hemoperfusion studies had focused on [36]. There are also some novel cytokines that can aggravate CKD such as tumorigenicity 1 and IL-8 in diabetic kidney disease [37,38]. IL-6, which had been proved is associated with mortality in incident dialysis patients [39] and PTH which is a key mediator of chronic kidney disease mineral and bone disorder [40] are involved in present study. Both 400/800 and 700/800 can absorb most IL-6 and PTH in blood samples of stage 5 CKD patients which indicated that they are ideal adsorbents for treatment of progressive CKD patients. According to above advantage, we also evaluated the toxin removal efficiency in simulated and in vivo hemoperfusion. As expected, as-prepared activated carbon can remove most of PR in simulated hemoperfusion, however, adsorbing material is loaded in a filter with small pore sizes which cannot support hemoperfusion at higher flush speed. To improve the hemoperfusion device, we used a filter contain the same membrane with clinical used hemoperfusion tank in the in vivo hemoperfusion test. The filter contains as-prepared material can work at 12 rpm for at least 15 min. After in vivo hemoperfusion using as-prepared activated carbon, blood Scr level of CKD rat was significantly decreased. Those results indicated that as-prepared activated carbons are valuable in treatment of CKD patients which can improve the hemoperfusion efficiency. Although our activated carbon can remove Scr in hemoperfusion of rats, filter used in the test still cannot support long-time hemoperfusion, to solve this problem, a bigger hemoperfusion filter is needed

if those activated carbons are further used in continuous hemoperfusion.

5. Conclusion

In summary, to increase the hemoperfusion efficiency, different kinds of porous biochar materials were synthesized via carbonization and activation of shell of areca nut at different temperatures. These porous biochar materials displayed good biocompatibility because of their low hemolysis rate. To demonstrate the feasibility and effectiveness of the materials derived from shell of areca nut as ideal adsorbents for hemoperfusion, the toxin removal efficiency of the as-prepared materials was evaluated. Owing to their porous structure and large surface area, the as-prepared materials could remove different toxins in solution, and their toxin removal efficiency is greater than that of TAC and commonly used reins. When added to the blood samples of CKD patients, IL-6, PTH and Scr were rapidly removed. Furthermore, IL-6 and Scr levels dramatically decreased after hemoperfusion using 400/800 and 700/800. According to the HE staining results, no apparent injury caused by hemoperfusion was observed in any of the different organs. The present study suggested that 400/800 and 700/800 are high-performance materials for hemoperfusion and hold great potential in the development of highly efficient adsorbents for clinical hemoperfusion therapy.

Ethics statement

All the experiments are approved by the Ethics Committee of the Affiliated Hospital of Qingdao University (AHQU-MAL2016016).

Data availability

The data that support the findings of this study are available from the corresponding author upon reasonable request.

CRediT authorship contribution statement

Chengyu Yang: Writing – original draft, Software, Project administration, Methodology, Investigation, Funding acquisition, Formal analysis, Data curation, Conceptualization. **Lipeng Diao:** Validation, Software, Resources. **Zhuo Song:** Methodology. **Chen Guan:** Software, Resources. **Lingyu Xu:** Validation. **Quandong Bu:** Supervision, Conceptualization. **Wei Jiang:** Visualization, Supervision, Data curation. **Huiqing Yu:** Visualization, Supervision, Data curation, Conceptualization. **Daohao Li:** Writing – review & editing, Supervision, Conceptualization. **Yan Xu:** Writing – review & editing, Supervision, Investigation, Funding acquisition, Data curation, Conceptualization.

Declaration of competing interest

The authors declare that they have no known competing financial interests or personal relationships that could have appeared to influence the work reported in this paper.

Acknowledgements

This work was supported by the National Natural Science Foundation of China (81970582 and 82270724), Medical Science and Technology Development Plan project of Shandong province (202103050716), Qingdao Key Health Discipline Development Fund, Qingdao Key Clinical Specialty Elite Discipline and Taishan Scholar Program of Shandong Province (NO.tstp20230665).

Appendix A. Supplementary data

Supplementary data to this article can be found online at https://doi.org/10.1016/j.heliyon.2024.e38892.

References

[1] J. Himmelfarb, R. Vanholder, The current and future landscape of dialysis [J] 16 (10) (2020) 573–585, https://doi.org/10.1038/s41581-020-0315-4.
[2] T. Liyanage, T. Ninomiya, V. Jha, B. Neal, H.M. Patrice, I. Okpechi, M.H. Zhao, J. Lv, A.X. Garg, J. Knight, A. Rodgers, M. Gallagher, S. Kotwal, A. Cass, V. Perkovic, Worldwide access to treatment for end-stage kidney disease: a systematic review, Lancet (London, England) 385 (9981) (2015) 1975–1982, https://doi.org/10.1016/s0140-6736(14)61601-9.
[3] N. Cai, Q. Li, J. Zhang, T. Xu, W. Zhao, J. Yang, L. Zhang, Antifouling zwitterionic hydrogel coating improves hemocompatibility of activated carbon hemoadsorbent, J. Colloid Interface Sci. 503 (2017) 168–177, https://doi.org/10.1016/j.jcis.2017.04.024.
[4] X. Song, K. Wang, C.Q. Tang, W.W. Yang, W.F. Zhao, Design of Carrageenan-Based Heparin-Mimetic Gel Beads as Self-Anticoagulant Hemoperfusion Adsorbents [J] 19 (6) (2018) 1966–1978, https://doi.org/10.1021/acs.biomac.7b01724.
[5] J. Zheng, L. Wang, X. Zeng, X. Zheng, Y. Zhang, S. Liu, X. Shi, Y. Wang, X. Huang, L. Ren, Controlling the integration of polyvinylpyrrolidone onto substrate by quartz crystal microbalance with dissipation to achieve excellent protein resistance and detoxification, ACS Appl. Mater. Interfaces 8 (29) (2016) 18684–18692, https://doi.org/10.1021/acsami.6b04348.

[6] R. Su, Y. Rao, X. Shen, J. Zhu, A. Ji, G. Jin, C. Dai, W. Hou, M. Yu, W. Lu, Preparation and adsorption properties of novel porous microspheres with different concentrations of bilirubin, Blood Purif. 42 (2) (2016) 104–110, https://doi.org/10.1159/000445933.

[7] W.K. Cheah, K. Ishikawa, R. Othman, F.Y. Yeoh, Nanoporous biomaterials for uremic toxin adsorption in artificial kidney systems: a review, J. Biomed. Mater. Res. B Appl. Biomater. 105 (5) (2017) 1232–1240, https://doi.org/10.1002/jbm.b.33475.

[8] S. Murugesan, T.J. Park, H. Yang, S. Mousa, R.J. Linhardt, Blood compatible carbon nanotubes–nano-based neoproteoglycans, Langmuir : the ACS journal of surfaces and colloids 22 (8) (2006) 3461–3463, https://doi.org/10.1021/la0534468.

[9] Q. Li, J. Yang, N. Cai, J. Zhang, T. Xu, W. Zhao, H. Guo, Y. Zhu, L. Zhang, Hemocompatible hemoadsorbent for effective removal of protein-bound toxin in serum, J. Colloid Interface Sci. 555 (2019) 145–156, https://doi.org/10.1016/j.jcis.2019.07.045.

[10] V. Wernert, O. Schäf, H. Ghobarkar, R. Denoyel, Adsorption properties of zeolites for artificial kidney applications, Microporous Mesoporous Mater. 83 (1) (2005) 101–113, https://doi.org/10.1016/j.micromeso.2005.03.018.

[11] J. Barnes, L.D. Cowgill, J. Diaz Auñon, Activated carbon hemoperfusion and plasma adsorption: rediscovery and veterinary applications of these abandoned therapies, Advances in Small Animal Care 2 (2021) 131–142, https://doi.org/10.1016/j.yasa.2021.07.010.

[12] L. Wu, L. Yang, A novel micro-sphere activated carbon synthesized from waste cigarette butts for ammonia adsorption, Waste Manag. 168 (2023) 396–405, https://doi.org/10.1016/j.wasman.2023.06.017.

[13] D. Angın, T.E. Köse, U. Selengil, Production and characterization of activated carbon prepared from safflower seed cake biochar and its ability to absorb reactive dyestuff, Appl. Surf. Sci. 280 (2013) 705–710, https://doi.org/10.1016/j.apsusc.2013.05.046.

[14] V.H. Nguyen, D.T. Nguyen, T.T. Nguyen, H.P.T. Nguyen, H.B. Khuat, T.H. Nguyen, V.K. Tran, S. Woong Chang, P. Nguyen-Tri, D.D. Nguyen, D.D. La, Activated carbon with ultrahigh surface area derived from sawdust biowaste for the removal of rhodamine B in water, Environ. Technol. Innovat. 24 (2021) 101811, https://doi.org/10.1016/j.eti.2021.101811.

[15] J. Luo, R. Yang, F. Ma, W. Jiang, C. Han, Recycling utilization of Chinese medicine herbal residues resources: systematic evaluation on industrializable treatment modes, Environ. Sci. Pollut. Res. Int. 30 (12) (2023) 32153–32167, https://doi.org/10.1007/s11356-023-25614-4.

[16] C. Huang, Z.X. Li, Y. Wu, Z.Y. Huang, Y. Hu, J. Gao, Treatment and bioresources utilization of traditional Chinese medicinal herb residues: recent technological advances and industrial prospect, J. Environ. Manag. 299 (2021) 113607, https://doi.org/10.1016/j.jenvman.2021.113607.

[17] P. Li, T. Zhao, Z. Zhao, H. Tang, W. Feng, Z. Zhang, Biochar Derived from Chinese Herb Medicine Residues for Rhodamine B Dye Adsorption [J] 8 (5) (2023) 4813–4825, https://doi.org/10.1021/acsomega.2c06968.

[18] R.J. Adam, A.C. Williams, A.J. Kriegel, Comparison of the surgical resection and infarct 5/6 nephrectomy rat models of chronic kidney disease [J] 322 (6) (2022), https://doi.org/10.1152/ajprenal.00398.2021. F639-f54.

[19] K.I. Greenberg, Choi, M.J. Hemodialysis Emergencies, Core curriculum 2021, Am. J. Kidney Dis. : the official journal of the National Kidney Foundation 77 (5) (2021) 796–809, https://doi.org/10.1053/j.ajkd.2020.11.024.

[20] J.I. Paredes, S. Villar-Rodil, A. Martínez-Alonso, J.M. Tascón, Graphene oxide dispersions in organic solvents, Langmuir : the ACS journal of surfaces and colloids 24 (19) (2008) 10560–10564, https://doi.org/10.1021/la801744a.

[21] J.H. Park, J.J. Wang, B. Zhou, J.E.R. Mikhael, R.D. Delaune, Removing mercury from aqueous solution using sulfurized biochar and associated mechanisms, Environmental pollution (Barking, Essex : 1987) 244 (2019) 627–635, https://doi.org/10.1016/j.envpol.2018.10.069.

[22] Y. Li, M. Biisembaev, Q. Gong, S. Aknazarov, F. Lu, Y. Huang, X. Zhao, K. Du, J. Bai, J. Gan, M. Zhao, D. Zhuang, Preparation of Lotus root-type monolithic-activated carbons with an hierarchical pore structure from rice husks and their adsorption of vitamin B12, ACS Omega 4 (20) (2019) 18930–18935, https://doi.org/10.1021/acsomega.9b03052.

[23] T.W. Meyer, J.L. Walther, M.E. Pagtalunan, A.W. Martinez, A. Torkamani, P.D. Fong, N.S. Recht, C.R. Robertson, T.H. Hostetter, The clearance of protein-bound solutes by hemofiltration and hemodiafiltration, Kidney Int. 68 (2) (2005) 867–877, https://doi.org/10.1111/j.1523-1755.2005.00469.x.

[24] T.W. Meyer, E.C. Leeper, D.W. Bartlett, T.A. Depner, Y.Z. Lit, C.R. Robertson, T.H. Hostetter, Increasing dialysate flow and dialyzer mass transfer area coefficient to increase the clearance of protein-bound solutes, J. Am. Soc. Nephrol. : JASN (J. Am. Soc. Nephrol.) 15 (7) (2004) 1927–1935, https://doi.org/10.1097/01.asn.0000131521.62256.f0.

[25] S. Magnani, M. Atti, Uremic toxins and blood purification: a review of current evidence and future perspectives, Toxins 13 (4) (2021), https://doi.org/10.3390/toxins13040246.

[26] T. Tang, X. Li, Y. Xu, D. Wu, Y. Sun, J. Xu, F. Deng, Bilirubin adsorption on amine/methyl bifunctionalized SBA-15 with platelet morphology, Colloids and surfaces B, Biointerfaces 84 (2) (2011) 571–578, https://doi.org/10.1016/j.colsurfb.2011.02.019.

[27] M. Ruospo, S.C. Palmer, P. Natale, J.C. Craig, M. Vecchio, G.J. Elder, G.F. Strippoli, Phosphate binders for preventing and treating chronic kidney disease-mineral and bone disorder (CKD-MBD), Cochrane Database Syst. Rev. 8 (8) (2018) Cd006023, https://doi.org/10.1002/14651858.CD006023.pub3.

[28] Y. Liu, X. Peng, Z. Hu, M. Yu, J. Fu, Y. Huang, Fabrication of a novel nitrogen-containing porous carbon adsorbent for protein-bound uremic toxins removal, Mater. Sci. Eng., C 121 (2021) 111879, https://doi.org/10.1016/j.msec.2021.111879.

[29] G. Batra, T. Ghukasyan Lakic, J. Lindbäck, C. Held, H.D. White, R.A.H. Stewart, W. Koenig, C.P. Cannon, A. Budaj, E. Hagström, A. Siegbahn, L. Wallentin, Interleukin 6 and cardiovascular outcomes in patients with chronic kidney disease and chronic coronary syndrome, JAMA cardiology 6 (12) (2021) 1440–1445, https://doi.org/10.1001/jamacardio.2021.3079.

[30] S.V. Mikhalovsky, Emerging technologies in extracorporeal treatment: focus on adsorption, Perfusion 18 (Suppl 1) (2003) 47–54, https://doi.org/10.1191/0267659103pf627oa.

[31] Y. Lu, Q. Gong, F. Lu, J. Liang, L. Ji, Q. Nie, X. Zhang, Preparation of sulfonated porous carbon nanotubes/activated carbon composite beads and their adsorption of low density lipoprotein, J. Mater. Sci. Mater. Med. 22 (8) (2011) 1855–1862, https://doi.org/10.1007/s10856-011-4368-6.

[32] D. Kong, G. Wang, Y. Tang, M. Guo, Z. Ul Haq Khan, Y. Guo, W. Gu, Y. Ma, M. Sui, J. Li, M. Yang, Potential health risk of areca nut consumption: hazardous effect of toxic alkaloids and aflatoxins on human digestive system, Food Res. Int. 162 (Pt A) (2022) 112012, https://doi.org/10.1016/j.foodres.2022.112012.

[33] I. Romero-Sánchez, E. Gracia-Lor, Y. Madrid-Albarrán, Aflatoxin detoxification by thermal cooking treatment and evaluation of in vitro bioaccessibility from white and brown rice, Food Chem. 436 (2024) 137738, https://doi.org/10.1016/j.foodchem.2023.137738.

[34] P. Evenepoel, P. Stenvinkel, Inflammation and gut dysbiosis as drivers of CKD-MBD [J] 19 (10) (2023) 646–657, https://doi.org/10.1038/s41581-023-00736-7.

[35] A. Petrazzuolo, G. Sabiu, E. Assi, A. Maestroni, I. Pastore, M.E. Lunati, L. Montefusco, C. Loretelli, G. Rossi, M. Ben Nasr, V. Usuelli, Y. Xie, H. B. Balasubramanian, M. Zocchi, B. El Essawy, J. Yang, F. D'addio, P. Fiorina, Broadening horizons in mechanisms, management, and treatment of diabetic kidney disease, Pharmacol. Res. 190 (2023) 106710, https://doi.org/10.1016/j.phrs.2023.106710.

[36] M.H. Rosner, T. Reis, Classification of Uremic Toxins and Their Role in Kidney Failure [J] 16 (12) (2021) 1918–1928, https://doi.org/10.2215/cjn.02660221.

[37] H. Kobayashi, H.C. Looker, E. Satake, Neuroblastoma suppressor of tumorigenicity 1 is a circulating protein associated with progression to end-stage kidney disease in diabetes [J] 14 (657) (2022) eabj2109, https://doi.org/10.1126/scitranslmed.abj2109.

[38] C. Loretelli, F. Rocchio, F. D'addio, M. Ben Nasr, E. Castillo-Leon, S. Dellepiane, A. Vergani, A. Abdelsalam, E. Assi, A. Maestroni, V. Usuelli, R. Bassi, I. Pastore, J. Yang, B. El Essawy, K.M. Elased, G.P. Fadini, E. Ippolito, A.J. Seelam, M. Pezzolesi, D. Corradi, G.V. Zuccotti, M. Gallieni, M. Allegretti, M.A. Niewczas, P. Fiorina, The IL-8-CXCR1/2 axis contributes to diabetic kidney disease, Metabolism: clinical and experimental 121 (2021) 154804, https://doi.org/10.1016/j.metabol.2021.154804.

[39] N. Roy, S.E. Rosas, IL-6 is associated with progression of coronary artery calcification and mortality in incident dialysis patients, Am. J. Nephrol. 52 (9) (2021) 745–752, https://doi.org/10.1159/000518652.

[40] E. Bellorin-Font, E. Rojas, K.J. Martin, Bone disease in chronic kidney disease and kidney transplant, Nutrients 15 (1) (2022), https://doi.org/10.3390/nu15010167.